COMMUNICATIONS IN NUMERICAL METHODS IN ENGINEERING

Commun. Numer. Meth. Engng 2000; **00**:1–6 *Prepared using* cnmauth.cls *[Version: 2002/09/18 v1.02]*

On Large Deformation Hyperelasto–Plasticity of Anisotropic Materials

Boris Jeremić (Борис Јеремић) [1] ,*

Zhao Cheng (程 昭) [2]

[1] *Associate Professor, Department of Civil and Environmental Engineering, University of California, Davis, CA 95616.* jeremic@ucdavis.edu

[2] *Staff Engineer, Earth Mechanics, Inc., Oakland, CA 94621*

KEY WORDS: anisotropy, hyperelastic-plastic, large deformations

SUMMARY

The main goal of this short paper is to bring forward and explore the issue of constitutive integrations in large deformation regime for anisotropic hyperelasto-plastic material models. Of particular interest is the appropriate treatment of cases with non–coaxiality of principal stress and its conjugate hyperelastic strain. The non–coaxiality can result from hyperelastic anisotropy, anisotropic flow directions or anisotropic yield function. In addition to discussing issues related to non–coaxiality,

*Correspondence to: Boris Jeremić, Department of Civil and Environmental Engineering, One Shields Ave., University of California, Davis, CA, 95616, U.S.A. jeremic@ucdavis.edu

Contract/grant sponsor: NSF; contract/grant number: EEC–9701568, CMS–0337811

a constitutive integration algorithm is presented in some detail that is designed to be applicable to anisotropic non–coaxial (as well as to isotropic) hyperelastic–plastic solids. A numerical example is used to illustrate the problem.

1. Introduction

The hyperelasto–plastic format mostly used today in large deformation computations is based on work by Simo and Ortiz [23], [21], Bathe et al. [1], Simo [24], [25], Eterovic and Bathe [5], Perić et al. [19] and Cuitino and Ortiz [4]. Earlier work on multiplicative split of the deformation gradient (Hill [8], Bilby et al. [2] Kröner [11], Lee and Liu [14], Fox [6] and Lee [13]) is incorporated in all the previous developments.

However, few researchers have addressed the issue of large-deformation hyperelastoplastic computational formulations for anisotropic materials. We mention an algorithm by Eterovic and Bathe [5] which is based on additive split of logarithmic stress and strain measures (elastic and hyperelastoplastic). They have also explored the use of a more general approximation of deformation tensors that can support both isotropic and anisotropic material models. More recently, Papadopoulos and Lu [17] developed a general framework for finite deformation elastoplasticity that is based on the early work of Green and Naghdi [7]. Developments include provisions for non-collinearity of principal stress and strain measures. The framework was tested using Von-Mises type yield criteria with translational kinematic hardening, which retain isotropy of yield and plastic potential functions. Somewhat similar developments were reported by Miehe et al. [15] and [16] . They used initial anisotropy in hyperelastic models and initially anisotropic criterion by Hill [8] to successfully simulate various problems. However, it was not

clear if, and how, the non–coaxiality of principal stress and its conjugate hyperelastic strain measures evolve and how much it influences the results.

Addressed here is the issue of non–coaxiality of principal stresses and its conjugate hyperelastic strains and its influence on large deformation hyperelastic–plastic integration algorithms. This non–coaxiality can stem from a number of features present in general hyperelastic–plastic material models. We list some of those features below:

Anisotropic Hyperelasticity: The non–coaxiality of principal stresses and its conjugate hyperelastic strains can result if the hyperelastic strain energy function is not an isotropic function of the elastic Euler-Green strain $\bar{b}^e_{ij}$ (or the elastic Lagrange-Green strain $\bar{C}^e_{ij}$). In the case that the yield function is an isotropic one as well, the assumption can be made that the elastic Euler–Green strain $\bar{b}^e_{ij}$ and the Kirchhoff stress τ_{ij} commute. This isotropic assumption makes basis for many previous developments (for example Simo [21], Simo and Miehe [22]). However, use of this assumption in developing consistent algorithms for large deformation hyperelastic–plastic response precludes them from being applied to anisotropic hyperelastic–plastic models. Our presented algorithm removes such limitation.

Non-isotropic Flow Rules: The non–coaxiality can result from the plastic flow rule that is not isotropic function of the Kirchhoff stress tensor τ_{ij}.

Kinematic Hardening: The non–coaxiality can develop if kinematic hardening is present. In that case, the induced anisotropy may destroy the isotropy of the yield function. One such simple example is that of von Mises model (yield function) with an initial back stress that is non–coaxial with the developing conjugate strain. Prevost [20] noted this case in

which the existence of kinematic hardening destroys the isotropy of the yield function. On the other hand, algorithms that assume that the yield function is an isotropic function of the Kirchhoff stress tensor τ_{ij} in order to satisfy the frame indifference cannot deal with this type of anisotropy.

Reversal of Loading, Cyclic loading: The non–coaxial may also occur during reversal of loading. That reversal of loading might change the ordering of three principal directions for stress and its conjugate hyperelastic strain independently, thus destroying coaxiality.

In what follows, a brief description of a generic version of hyperelastic–plastic material model is presented. Following that, the implicit algorithm is developed that resolves all the above mentioned issues with anisotropy. In addition to the fully implicit algorithm, presented is also the consistent tangent operator that is used in conjunction with global (finite element) level Newton iterations. A simple example which features a von Mises material model with initial back–stress is used to illustrate our approach.

2. General Anisotropic Hyperelasto–Plastic Models

In this section, an overview is made of a generic material model formulation that incorporates anisotropic feature described in the introduction. Material models incorporating described features are mostly found in dealing with continuum representation of particular materials (soils, rock, concrete, powders, bone material, foams...). A quite general description of any incremental material model can be done by separating the model into its components, namely (a) hyperelastic relations, (b) yield function, (c) flow rules and (d) hardening/softening laws.

Hyperelastic Relations The hyperelastic material derives from a general function Ψ which can be anisotropic, and relates the second Piola-Kirchhoff stress $\bar{S}_{ij}$ in the intermediate configuration and its conjugate elastic Green strain $\bar{E}^e_{ij}$:

$$\dot{\bar{S}}_{ij} = \bar{\mathcal{L}}_{ijkl}\dot{\bar{E}}^e_{kl} \quad ; \quad \bar{\mathcal{L}}_{ijkl} = \frac{\partial \bar{S}_{ij}}{\partial \bar{E}^e_{ij}} = \frac{\partial^2 \Psi}{\partial \bar{E}^e_{ij}\partial \bar{E}^e_{kl}} \tag{1}$$

where $\bar{\mathcal{L}}_{ijkl}$ is the Lagrange-Green stiffness tensor in the intermediate configuration, and $\bar{E}^e_{ij} := 1/2(\bar{C}^e_{ij} - \delta_{ij})$ is the elastic Lagrange–Green strain tensor, while $\bar{C}^e_{ij} := F^e_{ki}F^e_{kj}$ is the elastic Lagrange deformation tensor.

It proves convenient to define this relationship (Eq. 1) using Mandel stress $\bar{T}_{ij}(= \bar{C}^e_{ik}\bar{S}_{kj})$ and the elastic Green strain $\bar{E}_{ij}$, both in the intermediate configuration $\dot{\bar{T}}_{ij} = \bar{\mathcal{L}}^M_{ijmn}\dot{\bar{E}}^e_{mn}$ where $\bar{\mathcal{L}}^M_{ijmn} = \delta_{im}\bar{S}_{jn} + \delta_{in}\bar{S}_{jm} + \bar{C}^e_{ik}\bar{\mathcal{L}}_{kjmn}$ is the stiffness tensor connecting Mandel stress and Lagrange–Green strain tensors.

Yield Conditions The yield function can be expressed in terms of the Mandel stress in the intermediate configuration $\bar{T}_{ij}$, the scalar stress-like internal variable q, and the kinematic stress-like internal variable a_{ij} as

$$\mathscr{F} = \mathscr{F}(\bar{T}_{ij}, q, a_{ij}) = 0 \tag{2}$$

Since $\bar{T}_{ij}$ is invariant under any rigid translations or rotations, this yield function can represent any type of anisotropy.

Flow Rules The non–associated (or associated), anisotropic flow rule is defined in terms of the plastic deformation gradient as

$$\bar{L}^p_{ij} = \dot{F}^p_{ik}(F^p)^{-1}_{kj} = \dot{\lambda}\bar{M}_{ij}(\bar{T}_{ij}, q, a_{ij}) \tag{3}$$

where $\bar{M}_{ij}$ is the direction of plastic deformation. By using the definition for the plastic deformation rate ($\bar{l}^p_{ij} = \bar{C}^e_{ik}\bar{L}^p_{kj}$) and the symmetric part of the plastic deformation rate ($\bar{d}^p_{ij} = Sym(\bar{C}^e_{ik}\bar{L}^p_{kj})$), we obtain

$$\bar{d}^p_{ij} = \dot{\lambda}\bar{M}^C_{ij} \quad ; \quad \bar{M}^C_{ij} = Sym(\bar{C}^e_{ik}\bar{M}_{kj}) \tag{4}$$

For scalar (ξ) and kinematic (η_{ij}) internal variables, flow rules can be written as,

$$\dot{\xi} = -\dot{\lambda}\, n^{scalar}(\bar{T}_{ij}, q, a_{ij}) \quad ; \quad \dot{\eta}_{ij} = -\dot{\lambda}\, n^{kinematic}_{ij}(\bar{T}_{ij}, q, a_{ij}) \tag{5}$$

Hardening Laws The scalar and kinematic hardening laws are defined as

$$\dot{q} = K\dot{\xi} \quad ; \quad \dot{a}_{ij} = \mathcal{H}_{ijkl}\dot{\eta}_{kl} \tag{6}$$

where hardening/softening function $\mathcal{H}_{ijkl}$ can be any anisotropic function while K remains isotropic function.

3. Algorithmic Constitutive Formulation

In this section, a constitutive integration algorithm is developed that does not suffer from restrictions to isotropic material models (as described in the introductory section). It should be noted that in developments that follow, the Karush–Kuhn–Tucker (KKT) conditions $\dot{\lambda} \geq 0$, $\mathscr{F}(\bar{T}_{ij}, q, a_{ij}) \leq 0$ and $\dot{\lambda}\mathscr{F}(\bar{T}_{ij}, q, a_{ij}) = 0$ (Karush [10], Kuhn and Tucker [12]) which should be satisfied simultaneously, are used. In addition to KKT condition, consistency condition $\dot{\mathscr{F}}(\bar{T}_{ij}, q, a_{ij}) = 0$ is also enforced.

We start by integrating the flow rule (Equation (3)) from time step t to $t+1$ as

$${}^{n+1}F^p_{ij} = \exp\left(\Delta\lambda^{n+1}\bar{M}_{ik}\right){}^{n}F^p_{kj} \tag{7}$$

By using the multiplicative decomposition of the deformation gradient and Equation (7) we obtain

$$ {}^{n+1}F^{e}_{ij} = {}^{n+1}F_{im}\ \left({}^{n}F^{p}_{mk}\right)^{-1} \exp\left(-\Delta\lambda^{n+1}\bar{M}_{kj}\right) = {}^{n+1}\bar{F}^{e,trial}_{ik} \exp\left(-\Delta\lambda^{n+1}\bar{M}_{kj}\right) \tag{8} $$

where it was used that ${}^{n+1}F^{e,trial}_{ik} = {}^{n+1}F_{im}\ \left({}^{n}F^{p}_{km}\right)^{-1}$. The elastic deformation is then

$$ \begin{aligned} {}^{n+1}\bar{C}^{e}_{ij} &= \left({}^{n+1}F^{e}_{im}\right)^{T}\ {}^{n+1}\bar{F}^{e}_{mj} \\ &= \exp\left(-\Delta\lambda^{n+1}\bar{M}^{T}_{ir}\right)\ {}^{n+1}\bar{C}^{e,trial}_{rl}\ \exp\left(-\Delta\lambda^{n+1}\bar{M}_{lj}\right) \end{aligned} \tag{9} $$

By recognizing that the exponent of a tensor can be expanded in Taylor series (Pearson [18]),

$$ \exp\left(-\Delta\lambda^{n+1}\bar{M}_{lj}\right) = \delta_{lj} - \Delta\lambda^{n+1}\bar{M}_{lj} + Sym(\Delta\lambda^{n+1}\bar{M}_{ls}) + \cdots \tag{10} $$

and by applying first order expansion to Equation (9), and by neglecting the higher order terms (Jeremić et al. [9]) the solution for the right elastic deformation tensor ${}^{n+1}\bar{C}^{e}_{ij}$ can be written as

$$ {}^{n+1}\bar{C}^{e}_{ij} = {}^{n+1}\bar{C}^{e,trial}_{ij} - \Delta\lambda\ \left({}^{n+1}\bar{C}^{e,trial}_{ik}\ {}^{n+1}\bar{M}_{kj}\ + {}^{n+1}\bar{M}_{ik}\ {}^{n+1}\bar{C}^{e,trial}_{kj}\right) \tag{11} $$

It is important to note that the Taylor's series expansion from Equation 10 is a proper approximation for the general non-symmetric tensor $\bar{M}_{lj}$. That is, the approximate solution given by Equation 11 is valid for a general anisotropic solid.

The predictor–corrector relation for elastic Green strain can then be written as

$$ {}^{n+1}\bar{E}^{e}_{ij} = {}^{n+1}\bar{E}^{e,trial}_{ij} - \Delta\lambda\ \bar{M}^{C,trial}_{ij} \quad ; \quad \bar{M}^{C,trial}_{ij} = Sym({}^{n+1}\bar{C}^{e,trial}_{ik}\ {}^{n+1}\bar{M}_{kj}) \tag{12} $$

Similar predictor–corrector relations can be obtain for internal variables,

$$ {}^{n+1}\xi = {}^{n+1}\xi^{trial} - \Delta\lambda\ {}^{n+1}n^{scalar} \tag{13} $$

$$ {}^{n+1}\eta_{ij} = {}^{n+1}\eta^{trial}_{ij} - \Delta\lambda\ {}^{n+1}n^{kinematic}_{ij} \tag{14} $$

The iterative algorithm is then developed using a residual ${}^{n+1}\tilde{\mathbf{r}}_{\mathbf{A}}$ (using idea from Crisfield [3]) at step $n+1$

$$ {}^{n+1}\tilde{\mathbf{r}}_{\mathbf{A}} = {}^{n+1}\tilde{\mathbf{s}}_{\mathbf{A}} - \tilde{\mathbf{r}}_{\mathbf{A}}^{trial} + \Delta\lambda\, {}^{n+1}\tilde{\mathbf{m}}_{\mathbf{A}} \tag{15} $$

where $\tilde{\mathbf{r}}_A$, $\tilde{\mathbf{s}}_A$, and $\tilde{\mathbf{m}}_A$ are generalized vectors or matrices in which the element components are tensors and scalar:

$$ \tilde{\mathbf{r}}_{\mathbf{A}} = \left\{ \begin{array}{c} \bar{R}_{ij} \\ r^{scalar} \\ r_{ij}^{kinematic} \end{array} \right\}, \quad \tilde{\mathbf{s}}_{\mathbf{A}} = \left\{ \begin{array}{c} \bar{E}_{ij}^{e} \\ \xi \\ \eta_{ij} \end{array} \right\}, \quad \tilde{\mathbf{m}}_{\mathbf{A}} = \left\{ \begin{array}{c} \bar{M}_{ij}^{C} \\ n^{i} \\ n_{ij}^{k} \end{array} \right\} \tag{16} $$

Linearization of residual relation (Eq. (15)) while noting that trial variables are fixed during the iteration process and omitting the superscript $n+1$, yields

$$ \tilde{\mathbf{r}}_{\mathbf{A}}^{old} + \Delta^2\lambda\, \tilde{\mathbf{m}}_{\mathbf{A}} + \mathbb{C}_{\mathbf{AB}}^{-1}\Delta\tilde{\mathbf{s}}_{\mathbf{B}} = \mathbf{0} \tag{17} $$

where

$$ \mathbb{C}_{\mathbf{AB}} = \left[\begin{array}{ccc} I_{ijkl} + \Delta\lambda\dfrac{\partial\bar{M}_{ij}^{C}}{\partial\bar{T}_{mn}}\bar{\mathcal{L}}_{mnkl}^{M} & \Delta\lambda\dfrac{\partial\bar{M}_{ij}^{C}}{\partial q}K & \Delta\lambda\dfrac{\partial\bar{M}_{ij}^{C}}{\partial a_{mn}}\mathcal{H}_{mnkl} \\ \Delta\lambda\dfrac{\partial n^{scalar}}{\partial\bar{T}_{ij}}\bar{\mathcal{L}}_{ijkl}^{M} & 1 + \Delta\lambda\dfrac{\partial n^{scalar}}{\partial q}K & \Delta\lambda\dfrac{\partial n^{scalar}}{\partial a_{ij}}\mathcal{H}_{ijkl} \\ \Delta\lambda\dfrac{\partial n_{ij}^{kinematic}}{\partial\bar{T}_{mn}}\bar{\mathcal{L}}_{mnkl}^{M} & \Delta\lambda\dfrac{\partial n_{ij}^{kinematic}}{\partial q}K & I_{ijkl} + \Delta\lambda\dfrac{\partial n_{ij}^{kinematic}}{\partial a_{mn}}\mathcal{H}_{mnkl} \end{array} \right]^{-1} \tag{18} $$

and I_{ijkl} is the unit fourth order tensor.

The generalized matrix $\mathbb{C}$ has the following structure

$$ \mathbb{C} = \left[\begin{array}{ccc} \mathbb{C}^{\langle 11\rangle} & \mathbb{C}^{\langle 12\rangle} & \mathbb{C}^{\langle 13\rangle} \\ \mathbb{C}^{\langle 21\rangle} & \mathbb{C}^{\langle 22\rangle} & \mathbb{C}^{\langle 23\rangle} \\ \mathbb{C}^{\langle 31\rangle} & \mathbb{C}^{\langle 32\rangle} & \mathbb{C}^{\langle 33\rangle} \end{array} \right] \tag{19} $$

where $\mathbb{C}^{\langle 11\rangle}$, $\mathbb{C}^{\langle 13\rangle}$, $\mathbb{C}^{\langle 31\rangle}$, $\mathbb{C}^{\langle 33\rangle}$ are fourth order tensors, $\mathbb{C}^{\langle 12\rangle}$, $\mathbb{C}^{\langle 21\rangle}$, $\mathbb{C}^{\langle 23\rangle}$, $\mathbb{C}^{\langle 32\rangle}$ are second order tensors, and $\mathbb{C}^{\langle 22\rangle}$ is a scalar.

Linearized form of the consistency condition ${}^{n+1}\mathscr{F}\left({}^{n+1}\bar{T}_{ij}, {}^{n+1}q, {}^{n+1}a_{ij}\right) = 0$ at time $t+1$ yields

$$\tilde{\mathbf{f}}_{\mathbf{A}}^{T}\Delta\tilde{\mathbf{s}}_{\mathbf{A}} + \mathscr{F}^{old} = \mathbf{0} \tag{20}$$

where $\Delta\tilde{\mathbf{s}}_{\mathbf{A}}$ is the differential form of a generalized vector $\tilde{\mathbf{s}}_{\mathbf{A}}$ from Equation (16) and (generalized) vector $\tilde{\mathbf{f}}_{\mathbf{A}}$ is defined as

$$\tilde{\mathbf{f}}_{\mathbf{A}} = \left\{ \begin{array}{ccc} \dfrac{\partial\mathscr{F}}{\partial\bar{T}_{ij}}\bar{\mathcal{L}}^{M}_{ijkl} & \dfrac{\partial\mathscr{F}}{\partial q}K & \dfrac{\partial\mathscr{F}}{\partial a_{ij}}\mathcal{H}_{ijkl} \end{array} \right\}^{T} \tag{21}$$

By using Equations (17) and (20) one can solve for $\Delta\lambda$

$$\Delta^{2}\lambda = \frac{\mathscr{F}^{old} - \tilde{\mathbf{f}}_{\mathbf{A}}^{T}\mathbb{C}_{\mathbf{AB}}\tilde{\mathbf{r}}_{\mathbf{B}}}{\tilde{\mathbf{f}}_{\mathbf{C}}^{T}\mathbb{C}_{\mathbf{CD}}\tilde{\mathbf{m}}_{\mathbf{D}}} \tag{22}$$

which can be used in conjunction with Equation 17 to solve for an increment in (quasi) vector $\tilde{\mathbf{s}}_{\mathbf{A}}$

$$\Delta\tilde{\mathbf{s}}_{\mathbf{A}} = \left\{ \begin{array}{c} \Delta\bar{E}^{e}_{kl} \\ \Delta\xi \\ \Delta\eta_{kl} \end{array} \right\} = -\mathbb{C}_{\mathbf{AB}}\left(\tilde{\mathbf{r}}_{\mathbf{B}} + \Delta^{2}\lambda\,\tilde{\mathbf{m}}_{\mathbf{B}}\right) \tag{23}$$

that contains increments of elastic Green strain tensor ($\Delta\bar{E}^{e}_{ij}$, used to find Second Piola–Kirchhoff stress), scalar ($\Delta\xi$) and kinematic ($\Delta\eta_{ij}$) internal variables. Iterations continue until both consistency condition (${}^{n+1}\mathscr{F}\left({}^{n+1}\bar{T}_{ij}, {}^{n+1}q, {}^{n+1}a_{ij}\right) = 0$) and minimization of the norm of the residual ($\tilde{\mathbf{r}}_{\mathbf{A}} = 0$) are satisfied (within some tolerance).

In addition to the fully implicit algorithm, described above, the algorithmic, consistent stiffness tensor in intermediate configuration $\bar{\mathcal{L}}^{AS}_{ijmn}$ is derived similarly as

$$\bar{\mathcal{L}}^{AS}_{ijmn} = \bar{\mathcal{L}}_{ijkl}\hat{\mathbb{C}}^{\langle 11\rangle}_{klmn} \qquad \text{from} \qquad d\bar{S}_{ij} = \bar{\mathcal{L}}_{ijkl}d\bar{E}^{e}_{kl} = \bar{\mathcal{L}}_{ijkl}\hat{\mathbb{C}}^{\langle 11\rangle}_{klmn}d\bar{E}^{e,trial}_{mn} \tag{24}$$

where $\hat{\mathbb{C}}^{\langle 11\rangle}$ is the upper-left $(1,1)$ block of the generalized matrix of $\hat{\mathbb{C}}$,

$$\hat{\mathbb{C}}_{\mathbf{AB}} := \mathbb{C}_{\mathbf{AB}} - \frac{(\mathbb{C}_{\mathbf{AM}}\tilde{\mathbf{m}}_{\mathbf{M}})(\tilde{\mathbf{f}}_{\mathbf{N}}^{T}\mathbb{C}_{\mathbf{NB}})}{\tilde{\mathbf{f}}_{\mathbf{C}}^{T}\mathbb{C}_{\mathbf{CD}}\tilde{\mathbf{m}}_{\mathbf{D}}} \tag{25}$$

and $\tilde{\mathbf{m}}_{\mathbf{M}}$, $\mathbb{C}_{\mathbf{AM}}$ and $\tilde{\mathbf{f}}^{T}_{\mathbf{N}}$ were defined by equations (16), (18) and (21).

The algorithmic stiffness tensor is used on the finite element level to provide for fast (quadratic once within Newton trust region) convergence.

4. Numerical Example

A numerical example with non-coaxial anisotropic model is used to demonstrated described developments. Material model is an extension of von Mises yield and potential surfaces with kinematic hardening. The kinematic hardening features initial back stress (which might have developed from previous (cyclic) loading stage) that is not coaxial with the developing conjugate hyperelastic strain. This non–coaxiality will in this case prevent use of any constitutive integration algorithms that is relying on assumption of coaxiality of stress and its conjugate hyperelastic strain.

The material model yield function is defined as

$$\mathscr{F}(\tau_{ij}, a_{ij}) = \frac{3}{2}(Dev(\tau_{ij}) - x_{ij} - a_{ij})(Dev(\tau_{ij}) - x_{ij} - a_{ij}) - Y_0^2 = 0 \tag{26}$$

where $Dev(\tau_{ij})$ is the deviatoric part of Kirchhoff stress in the current configuration. The material constant Y_0 represents the yield strength, while x_{ij} represents constant back stress tensor, and a_{ij} is the kinematic hardening (internal variable, stress-like) tensor. It is easy to obtain the first derivative of the yield function with respect to Kirchhoff stress as

$$\frac{\partial \mathscr{F}}{\partial \tau_{ij}} = 3[Dev(\tau_{ij}) - x_{ij} - a_{ij}] \tag{27}$$

If x_{ij} is zero tensor, Kirchhoff stress τ_{ij} and first derivatives of yield function $\partial\mathscr{F}/\partial\tau_{ij}$ are co-axial. However, if x_{ij} is any non–zero tensor (except for pure hydrostatic tensor, like Kronecker delta δ_{ij}), then the Kirchhoff stress τ_{ij} and and derivatives of yield function $\partial\mathscr{F}/\partial\tau_{ij}$ are not

coaxial. It should be noted that the yield function given in Equation (26) is defined in terms of Kirchhoff stress, while it will be redefined (in the same form) in terms of the Mandel stress $\bar{T}_{ij}$ in the intermediate configuration in order to use it in developed algorithms.

The hyperelasticity is of compressible Neo-Hookean type with the strain energy function given as

$$\Psi = \frac{1}{2}\lambda_0 \left(\ln J\right)^2 - G_0(\ln J) + \frac{1}{2}G_0 \left(tr(\bar{C}^e) - 3\right) \tag{28}$$

where G_0 is shear modulus and $\lambda_0 = K_0 - (2/3)G_0$ is Lamé constant while K_0 is bulk modulus. Volume ration J is defined as $J^2 = \det(\bar{C}^e_{ij})$ while trace of the elastic Lagrange-Green strain is $tr(\bar{C}^e_{ij}) = \bar{C}^e_{ii}$. The material constants are $K_0 = 1971.67$ kPa, $G_0 = 4225.50$ kPa, $Y_0 = 10$ kPa, while linear kinematic hardening law is adopted with hardening modulus $H = 80$ kPa.

A random non–zero tensor x_{ij} can be used to show non–coaxiality, but here, without losing generality, x_{ij} is given as

$$x_{ij} = \begin{bmatrix} 0.0 & 0.0 & 0.0 \\ 0.0 & 0.0 & x \\ 0.0 & x & 0.0 \end{bmatrix} \tag{29}$$

where x is a given scalar controlling the size of the back stress and has units of stress. The deformation is defined through a simple deformation gradient for simple shear given as

$$F_{ij} = \begin{bmatrix} 1.0 & 0.0 & \gamma \\ 0.0 & 1.0 & 0.0 \\ 0.0 & 0.0 & 1.0 \end{bmatrix} \tag{30}$$

where γ is the shear ratio.

In this example, a total of 100 increments $\Delta\gamma = 0.05\%$ are used. The eigenvectors of the left Cauchy–Green deformation b_{ij} and the Cauchy stress σ_{ij} ($\sigma_{ij} = J\tau_{ij}$, so that σ_{ij} and τ_{ij} are

always coaxial) are compared for collinearity. Table I list those eigenvectors at $\gamma = 5\%$ with initial non–zero and zero back stress as expressed in Equation (29). It is obvious that for the non–zero back stress (anisotropic case) that the eigenvectors of b_{ij} and σ_{ij} are non-coaxial. On the other hand, for zero back stress (isotropic case) the eigenvectors are equal, that is, the stress and strain tensors are coaxial. It follows that with even simple non–coaxial material

Table I. Calculated eigenvectors (EV) at shear deformation of $\gamma = 5\%$ for non–coaxial ($x = 5.0$ kPa) and coaxial ($x = 0.0$ kPa) cases.

	non–coaxial, $x = 5.0$ kPa			coaxial, $x = 0.0$ kPa		
	EV 1	EV 2	EV 3	EV 1	EV 2	EV 3
b_{ij}	0.71589	0.00000	-0.69822	0.71589	0.00000	-0.69822
	0.00000	1.00000	0.00000	0.00000	1.00000	0.00000
	0.69822	0.00000	0.71589	0.69822	0.00000	0.71589
σ_{ij}	0.64279	-0.43400	-0.63124	0.71589	0.00000	-0.69822
	0.31581	0.90088	-0.29780	0.00000	1.00000	0.00000
	0.69792	-0.00794	0.71613	0.69822	0.00000	0.71589

model the constitutive integrations cannot use any of the algorithms that make coaxiality (of stress and its conjugate hyperelastic strain, and/or stress and the gradient of yield function in stress space) assumption. Rather, integration algorithms that take non–coaxiality into account, like the one described above, need to be used.

It is also interesting to compare results for shearing of material models with back stress that is (a) coaxial (using $x = 0.0$) and (b) non–coaxial (using $x = 5.0$). Such results, (σ_{13} versus γ) are presented in Figure 1(A). The response of the coaxial linear kinematic hardening

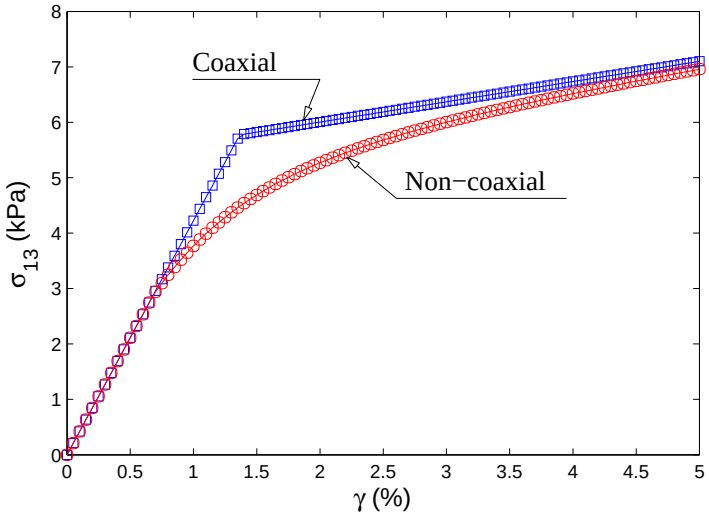

Figure 1. Simulation results (γ versus σ_{13}) for material model with (a) coaxial (using $x = 0.0$) and (b) non–coaxial (using $x = 5.0$) back stress.

material model (with $x = 0.0$ kPa) is represented by a bilinear response (as expected). On the other hand, the response of the similar material model with initial back stress ($x = 5.0$ kPa), is nonlinear from the moment it yields. This is also expected as the initial back stress is applied to different component ($x_{23} = x_{32} = 5.0$ kPa) than the one which is loaded (F_{13}). The yielding also happens sooner as the yield surface is shifted toward stress origin by the presence of the initial back stress. The nonlinearity of response follows from the fact that the yield and potential surfaces harden according to Prager's rule, following the increment of plastic deformation, which now changes non–linearly as there was a shift (initial back stress) in position of those two surfaces.

5. Summary

This short paper brings forward the issue of constitutive integration for large deformation hyperelastic–plastic material models which develop non–coaxiality of principal stress and its conjugate hyperelastic strain. In addition to discussion on non–coaxiality, briefly described was a constitutive integration algorithm that resolve the limitations to hyperelastic isotropy, plastic flow direction isotropy and yield function isotropy. A simple example was used to illustrate discussed issues through an anisotropic model with initial back–stress and its constitutive integration.

REFERENCES

1. K.J. Bathe, R. Slavković, and M. Kojić. On large strain elasto–plastic and creep analysis. In Wunderlich Bergan, Bathe, editor, *Finite Element Methods for Nonlinear Problems, Europe–US Symposium, Trondheim, Norway*, pages 176–190, 1985.
2. B. A. Bilby, L. R. T. Gardner, and A. N. Stroh. Continuous distributions of dislocations and the theory of plasticity. In IX^e *Congrès International de Mèchanique Appliquèe*, volume VIII, pages 35–44, Universitè de Bruxelles, 50. Avènue Franklin Roosevelt, 1957.
3. M. A. Crisfield. *Non–Linear Finite Element Analysis of Solids and Structures Volume 1: Advanced Topics*. John Wiley and Sons, Inc. New York, 605 Third Avenue, New York, NY 10158–0012, USA, 1997.
4. A. Cuitiño and M. Ortiz. A material – independent method for extending stress update algorithms from small–strain plasticity to finite plasticity with multiplicative kinematics. *Engineering Computations*, 9:437–451, 1992.
5. Adrian Luis Eterovic and Klaus-Jürgen Bathe. A hyperelastic – based large strain elasto – plastic constitutive formulation with combined isotropic – kinematic hardening using the logarithmic stress and strain measures. *International Journal for Numerical Methods in Engineering*, 30:1099–1114, 1990.
6. N. Fox. On the continuum theories of dislocations and plasticity. *Quarterly Journal of Mechanics and Applied Mathematics*, XXI(1):67–75, 1968.

7. A. Green and P Naghdi. A general theory of an elastic-plastic continuum. *Arch Rational Mechanical Analysis*, 18:251–281, 1965.

8. R. Hill. *The Mathematical Theory of Plasticity*. The Oxford Engineering Science Series. Oxford at the Clarendon Press, 1st. edition, 1950.

9. Boris Jeremić, Kenneth Runesson, and Stein Sture. A model for elastic–plastic pressure sensitive materials subjected to large deformations. *International Journal of Solids and Structures*, 36(31/32):4901–4918, 1999.

10. W. Karush. Minima of functions of several variables with inequalities as side constraints. Master's thesis, University of Chicago, Chicago, IL., 1939.

11. Ekkehart Kröner. Algemeine kontinuumstheorie der versetzungen und eigenspanungen. *Archive for Rational Mechanics and Analysis*, 4(4):273–334, 1960.

12. H. W. Kuhn and A. W. Tucker. Nonlinear programming. In Jerzy Neyman, editor, *Proceedings of the Second Berkeley Symposium on Mathematical Statistics and Probability*, pages 481 – 492. University of California Press, July 31 – August 12 1950 1951.

13. E. H. Lee. Elastic–plastic deformation at finite strains. *Journal of Applied Mechanics*, 36(1):1–6, 1969.

14. E. H. Lee and D. T. Liu. Finite–strain elastic–plastic theory with application to plane–wave analysis. *Journal of Applied Physics*, 38(1):19–27, January 1967.

15. C. Miehe, N. Apel, and M. Lambrecht. Anisotropic additive plasticity in the logarithmic strain space: modular kinematic formulation and implementation based on incremental minimization principles for standard materials. *Computer Methods in Applied Mechanics and Engineering*, 191:5383–5425, 2002.

16. Christian Miehe and Nikolas Apel. Anisotropic elastic-plastic analysis of shells at large strains. a comparison of multiplicative and additive approaches to enhanced finite element design and constitutive modelling. *International Journal for Numerical Methods in Engineering*, 61(12):2067 – 2113, 2004.

17. Panayaiotis Papadopoulos and Jia Lu. A general framework for the numerical solution of problems in finite elasto-plasticity. *International Journal for Computer Methods in Applied Mechanics and Engineering*, 159:1–18, 1998.

18. Carl E. Pearson, editor. *Handbook of Applied Mathematics*. Van Nostrand Reinhold Company, 1974.

19. Djordje Perić, D. R. J. Owen, and M. E. Honnor. A model for finite strain elasto–plasticity based on logarithmic strains: Computational issues. *Computer Methods in Applied Mechanics and Engineering*, 94:35–61, 1992.

20. Jean H. Prevost. Modeling the behavior of geomaterial. In Sayed M. Sayed, editor, *Geotechnical Modeling*

and Applications, pages 8–75. Gulf Publishing Company, Houston, London, Paris, Tokyo, 1987.

21. J. C. Simo. Algorithms for static and dynamic multiplicative plasticity that preserve the classical return mapping schemes of the infinitesimal theory. *Computer Methods in Applied Mechanics and Engineering*, 99:61–112, 1992.
22. J. C. Simo and C. Miehe. Associative coupled thermoplasticity at finite strains: Formulation, numerical analysis and implementation. *Computer Methods in Applied Mechanics and Engineering*, 98:41–104, 1992.
23. J. C. Simo and M. Ortiz. A unified approach to finite deformation elastoplastic analysis based on the use of hyperelastic constitutive equations. *Computer Methods in Applied Mechanics and Engineering*, 49:221–245, 1985.
24. Juan C. Simo. A framework for finite strain elastoplasticity based on maximum plastic dissipation and the multiplicative decomposition: Part i. continuum formulation. *Computer Methods in Applied Mechanics and Engineering*, 66:199–219, 1988. TA345. C6425.
25. Juan C. Simo. A framework for finite strain elastoplasticity based on maximum plastic dissipation and the multiplicative decomposition: Part ii. computational aspects. *Computer Methods in Applied Mechanics and Engineering*, 68:1–31, 1988. TA345. C6425.

